QED x QCD matching between the $\overline{\text{MS}}$ and the RI schemes

Based on JHEP01(2023)159

Francesco Moretti
In collaboration with M. Gorbahn, S. Jäger, E. van der Merwe

University of Liverpool

UKLFT Annual Meeting
University of Cambridge, 27 March 2023

Outline

Introduction

- Precise determination of lattice form factors requires a systematic treatment of QED corrections $\rightarrow$ perturbative matching to continuum renormalisation schemes.

- $\mathcal{O}(\alpha)$ matching between the $\mathrm{RI}'\text{-}\mathrm{MOM}$ scheme and the W-Mass scheme in [Di Carlo *et al.*, 2019].

- In this talk I will present our newly derived $\overline{\mathrm{RI}}\text{-}\mathrm{MOM}$ scheme and relative results for the conversion to the $\overline{\mathrm{MS}}$ at $\mathcal{O}(\alpha\ \alpha_s)$.

Outline

Lattice Renormalisation

- $O_{sem}(x) = \bar{d}(x)\gamma^\mu P_L u(x) \otimes \bar{\nu}_l(x)\gamma_\mu P_L l(x), \quad P_L = (1-\gamma^5)/2$

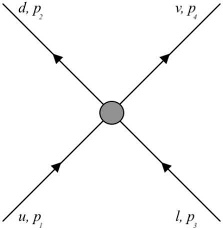

Figure: Kinematic conventions for the four-point diagrams.

- RI′-MOM [Martinelli *et al.*, 1995] (**This talk's focus**)

$$p_1 = p_2 = p_3 = p_4 = p, \quad p^2 = -\mu^2;$$

- RI-SMOM [Sturm *et al.*, 2009] (main paper for details)

$$p_1 = p_3, \quad p_2 = p_4, \quad p_1^2 = p_2^2 = -\mu^2, \quad p_1 \cdot p_2 = -\frac{1}{2}\mu^2.$$

Lattice Renormalisation

- Off-shell renormalisation conditions and the projector $\mathcal{P}$ define the RI schemes

$$\sigma_f^A \equiv \frac{1}{4\,p^2}\mathrm{Tr}(S_{f,\,A}^{-1}(p)\not{p}) \overset{A=\mathrm{RI}}{=} 1, \quad \lambda^A \equiv \Lambda^A_{\alpha\beta\gamma\delta}\mathcal{P}^A_{\alpha\beta\gamma\delta} \overset{A=\mathrm{RI}}{=} 1.$$

- The scheme conversion factors are

$$\mathcal{C}_f^{\overline{\mathrm{MS}}\to RI} = \left(\sigma_f^{\overline{\mathrm{MS}}}\right)^{-1/2}, \quad \mathcal{C}_O^{\overline{\mathrm{MS}}\to RI} = \lambda^{\overline{\mathrm{MS}}}\left(\sigma_u^{\overline{\mathrm{MS}}}\sigma_d^{\overline{\mathrm{MS}}}\sigma_\ell^{\overline{\mathrm{MS}}}\right)^{1/2}.$$

- Crucial role of $\mathcal{P}$ $\to$ What is a “good” projector?

- Conventionally [Garron, 2018], $\mathcal{P}^{\mathrm{RI'\text{-}MOM}} = -\frac{1}{16}\left(\gamma^\mu P_R \otimes \gamma_\mu P_R\right)$.

- Non-trivial renormalisation of conserved current $\to$ scale dependence of the conversion factor already in pure QCD.

Lattice Renormalisation

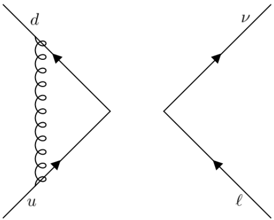

Figure: One-loop pure QCD correction.

- Neglecting QED $\to \Lambda^b = \Lambda^{b,\mu}(p) \otimes \gamma_\mu P_L + \mathcal{O}(\alpha)$, where $\Lambda^{b,\mu}(p) = F_1(p)\gamma^\mu P_L + F_2(p)\frac{p^\mu \not{p}}{p^2} P_L$.
- Ward Identity: $\Lambda^{b,\mu}(p) = \frac{\partial}{\partial p_\mu} S^b(\not{p})^{-1} \to F_1(p) = S^{-1}(p^2)$.
- $Z_{OO}^{\overline{\mathrm{MS}}} = 1 + \mathcal{O}(\alpha)$ & $Z_{OO}^{\mathrm{RI'\text{-}MOM}} = 1 + \mathcal{O}(\alpha_s)$.

Lattice Renormalisation

- Imposing $\mathcal{P}(\gamma^\mu P_L \otimes \gamma_\mu P_L) = 1$ and $\mathcal{P}(\frac{p^\mu \not{p}}{p^2} P_L \otimes \gamma_\mu P_L) = 0 \rightarrow$ $\mathcal{P}^{\overline{\mathrm{RI}}\text{-}\mathrm{MOM}} = -\frac{1}{12\, p^2}\left(\not{p} P_R \otimes \not{p} P_R + \frac{p^2}{2} \gamma^\nu P_R \otimes \gamma_\nu P_R\right)$.

- In this newly derived scheme $\rightarrow Z_{OO}^{\overline{\mathrm{RI}}\text{-}\mathrm{MOM}} = 1 + O(\alpha)$.

- No artificial scale dependence when the perturbative matching to continuum schemes is performed.

- Similar results for SMOM kinematics are presented in our work.

Outline

Results

RI′-MOM Wilson Coefficient

$$C_O^{\mathrm{RI'\text{-}MOM}}(\mu_L, p^2) = C_\alpha^{\mathrm{RI'\text{-}MOM}} + C_{\alpha_s}^{\mathrm{RI'\text{-}MOM}} + \frac{\alpha}{4\pi}\left(C_{\alpha,\alpha_s\, LL}^{\mathrm{RI'\text{-}MOM}} + C_{\alpha,\alpha_s\, NLL}^{\mathrm{RI'\text{-}MOM}}\right)$$

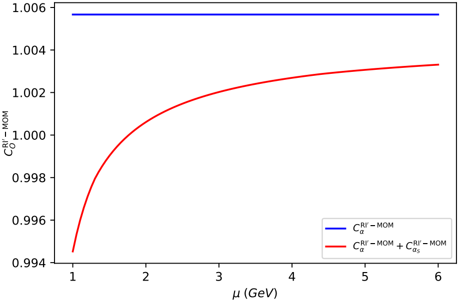

Figure: Residual μ-dependence of the low-scale Wilson coefficient $C_O^{\mathrm{RI'\text{-}MOM}}(\mu_L, p^2 = -9)$. It is evident that the leading strong corrections introduce an artificial scale dependence at low scales $\mu \sim \mu_L$.

Results

$\overline{\mathrm{RI}}$-MOM Wilson Coefficient

$$C_O^{\overline{\mathrm{RI}}\text{-MOM}}(\mu_L, p^2) = C_\alpha^{\overline{\mathrm{RI}}\text{-MOM}} + \frac{\alpha}{4\pi}\left(C_{\alpha,\alpha_s\, LL}^{\overline{\mathrm{RI}}\text{-MOM}} + C_{\alpha,\alpha_s\, NLL}^{\overline{\mathrm{RI}}\text{-MOM}}\right)$$

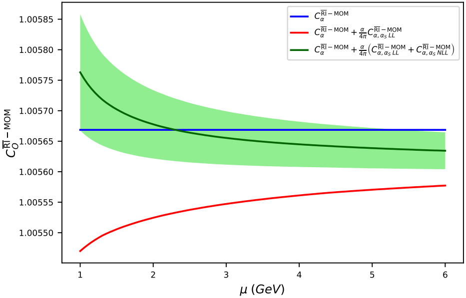

Figure: Scale dependence of $C_O^{\overline{\mathrm{RI}}\text{-MOM}}(\mu_L, p^2 = -9)$. The boundaries of the light green shaded area are obtained with different values of the three-loops operator's anomalous dimension $\gamma_O^{(2)}$: $\gamma_O^{(2)}$=-100 (top) and $\gamma_O^{(2)}$=100 (bottom). The dark green curve is obtained with $\gamma_O^{(2)} = 0$.

Outline

Ongoing Work & Future Outlooks

- We derived the two-loops $O(\alpha\ \alpha_s)$ $\overline{\mathrm{MS}}$ Wilson Coefficient at the high scale

$$C_O^{\overline{\mathrm{MS}}}(\mu_W, M_Z) = \frac{\alpha_s(\mu_W)}{4\pi}\frac{\alpha}{4\ \pi} C_F \left(3\left(\ln\left(\frac{\mu_W}{M_Z}\right)\right.\right.$$
$$\left.\left. - \csc^2(\theta_W)\left(\cot^2(\theta_W)\ln\left(\frac{M_W}{M_Z}\right)+1\right)\right) + \frac{95}{24}\right)$$

- Currently working on the derivation of the three-loops $O(\alpha\ \alpha_s^2)$ anomalous dimension $\gamma_O^{(2)}$.

- Phenomenological application of our results, e.g. CKM matrix elements extraction.

Ongoing Work & Future Outlooks

- We derived the two-loops $O(\alpha\ \alpha_s)$ $\overline{\mathrm{MS}}$ Wilson Coefficient at the high scale

$$C_O^{\overline{\mathrm{MS}}}(\mu_W, M_Z) = \frac{\alpha_s(\mu_W)}{4\pi}\frac{\alpha}{4\ \pi} C_F \left(3\left(\ln\left(\frac{\mu_W}{M_Z}\right)\right.\right. \\ \left.\left. - \csc^2(\theta_W)\left(\cot^2(\theta_W)\ln\left(\frac{M_W}{M_Z}\right)+1\right)\right) + \frac{95}{24}\right)$$

- Currently working on the derivation of the three-loops $O(\alpha\ \alpha_s^2)$ anomalous dimension $\gamma_O^{(2)}$.

- Phenomenological application of our results, e.g. CKM matrix elements extraction.

- **Thank You!**

Backup Slides

W-Mass

- The W-Mass renormalization scheme was traditionally used in the determination of the Fermi constant G_F [Sirlin, 1978] and is still in use in the calculation of electroweak corrections for the semi-leptonic decays [Seng *et al.*, 2020]

$$\frac{1}{q^2} \to \frac{1}{q^2 - M_W^2} + \frac{M_W^2}{M_W^2 - q^2}\frac{1}{q^2}$$

- The $\mathcal{O}(\alpha)$ matching between $\mathrm{RI'\text{-}MOM}$ and W-Mass was given in [Di Carlo *et al.*, 2019].

- We believe that the $\overline{\mathrm{MS}}$, where an EFT framework for EW corrections is very well established, allows for a better scale separation.

EFT Approach

- $\overbrace{\lambda^i(\mu_L, p^2)\, \mathcal{C}_O^{\overline{\mathrm{MS}}\to i}}^{\text{low}-\text{scale}}\; \overbrace{\mathcal{U}(\mu_L, \mu_W)\; C_O^{\overline{\mathrm{MS}}}(\mu_W, M_Z)}^{\text{high}-\text{scale}} \to$ scale independent.

- RI Wilson Coefficient:
  $C_O^{\mathrm{RI}}(\mu_L, p^2) = \mathcal{U}(\mu_L, \mu_W)\; C_O^{\overline{\mathrm{MS}}}(\mu_W, M_Z)\; \mathcal{C}_O^{\overline{\mathrm{MS}}\to \mathrm{RI}}(\mu_L, p^2) =$
  $C_\alpha^{\mathrm{RI}} + C_{\alpha_s}^{\mathrm{RI}} + \frac{\alpha}{4\pi}\left(C_{\alpha,\alpha_s\; LL}^{\mathrm{RI}} + C_{\alpha,\alpha_s\; NLL}^{\mathrm{RI}}\right)$

- C_α^{RI} and $C_{\alpha_s}^{\mathrm{RI}}$ are the resummed QED and leading QCD contributions. Neglecting threshold corrections
  $C_{\alpha,\alpha_s LL}^{\mathrm{RI}} = -\frac{\gamma_O^{(1)}}{2\beta_{(0)}^{(5)}} \ln\left(\frac{\alpha_s(\mu_L)}{\alpha_s(\mu_W)}\right),\; C_{\alpha,\alpha_s NLL}^{\mathrm{RI}} = \frac{\alpha_s(\mu_L)}{4\pi}\left(\mathcal{C}_O^{es}(-p^2, \mu_L^2) + \bar{\gamma}^{(5)}\right)$
  $+\frac{\alpha_s(\mu_W)}{4\pi}\left(C_O^{es}(\mu_W, M_Z) - \bar{\gamma}^{(5)}\right), \quad \bar{\gamma}^{(N_f)} = \frac{1}{2\beta_0^{(N_f)}}\left(\gamma_O^{(1)}\, \frac{\beta_1^{(N_f)}}{\beta_0^{(N_f)}} - \gamma_O^{(2)}\right)$

- Systematic inclusion of higher order corrections.

$\overline{\text{RI}}$-SMOM

- In the case of SMOM kinematics, the decomposition of the vertex function $\Lambda^{b,\mu}(p_1, p_2)$ is more complicated

$$\mathcal{T}_{(1)}(p_1,p_2) = \gamma^\mu P_L,\ \mathcal{T}_{(2)}(p_1,p_2) = \frac{1}{\mu^2}\not{p}_1 p_1^\mu P_L,$$
$$\mathcal{T}_{(3)}(p_1,p_2) = \frac{1}{\mu^2}\not{p}_1 p_2^\mu P_L,\ \mathcal{T}_{(4)}(p_1,p_2) = \frac{1}{\mu^2}\not{p}_2 p_1^\mu P_L,$$
$$\mathcal{T}_{(5)}(p_1,p_2) = \frac{1}{\mu^2}\not{p}_2 p_2^\mu P_L,\ \mathcal{T}_{(6)}(p_1,p_2) = \frac{1}{\mu^2}\gamma^\mu \not{p}_2 \not{p}_1 P_L.$$

- Imposing the relations that follows the WI we get
$\mathcal{P}^{\mathrm{RI/SMOM}} = \frac{1}{4}\Big(-\frac{1}{2}\gamma^\nu P_R \otimes \gamma_\nu P_R + \frac{1}{p^2}\not{p}_1 P_R \otimes \not{p}_1 P_R$
$+\frac{1}{p^2}\not{p}_2 P_R \otimes \not{p}_2 P_R - \frac{1}{p^2}\not{p}_1 P_R \otimes \not{p}_2 P_R - \frac{1}{p^2}\not{p}_2 P_R \otimes \not{p}_1 P_R\Big).$

$\overline{\mathrm{RI}}$-SMOM

$\overline{\mathrm{RI}}$-SMOM Wilson Coefficient:

$$C_O^{\overline{\mathrm{RI}}\text{-SMOM}}(\mu_L, p^2) =$$
$$\mathcal{U}(\mu_L, \mu_W)\ C_O^{\overline{\mathrm{MS}}}(\mu_W, M_Z)\ \mathcal{C}_O^{\overline{\mathrm{MS}}\to\overline{\mathrm{RI}}\text{-SMOM}}(\mu_L, p^2) =$$
$$C_\alpha^{\overline{\mathrm{RI}}\text{-SMOM}} + \frac{\alpha}{4\pi}\left(C_{\alpha,\alpha_s\ LL}^{\overline{\mathrm{RI}}\text{-SMOM}} + C_{\alpha,\alpha_s\ NLL}^{\overline{\mathrm{RI}}\text{-SMOM}}\right)$$

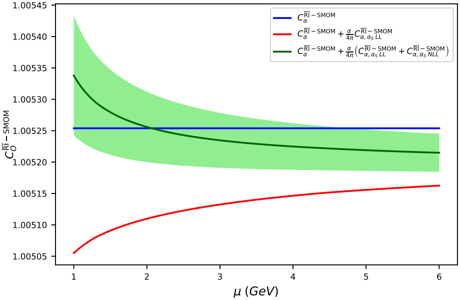

Figure: Scale dependence of $C_O^{\overline{\mathrm{RI}}\text{-SMOM}}(\mu_L, p^2 = -9)$. The boundaries of the light green shaded area are obtained with different values of the three-loops operator's anomalous dimension $\gamma_O^{(2)}$: $\gamma_O^{(2)}$=-100 (top) and $\gamma_O^{(2)}$=100 (bottom). The dark green curve is obtained with $\gamma_O^{(2)} = 0$.